J Therm Anal Calorim
DOI 10.1007/s10973-015-4945-x

Inclusion of prednicarbate in the SBA-15 silica

Protective effect and analytical profile when incorporated in a semisolid pharmaceutical formulation

Hélio Salvio Neto[1] · Gabriel Lima Barros de Araujo[1] · Leandro Luiz dos Santos[2] · Ivana Conte Cosentino[3] · Flávio Machado de Souza Carvalho[4] · Jivaldo do Rosário Matos[5]

Received: 1 May 2015 / Accepted: 21 July 2015

Abstract The present work describes the development and characterization of a nanostructured mesoporous SBA-15 silica loaded with prednicarbate, a corticosteroid widely used in the treatment for atopic dermatitis, and the assessment of its in vitro release profile in comparison with a conventional cream formulation. The inclusion of prednicarbate in the SBA-15 pores was confirmed by the respective 24 and 16 % decrease in the surface area (S_{BET}) and mesopores volume (V), in combination with supporting data obtained by thermal analysis (TG and DSC), FTIR spectroscopy, X-ray diffraction, and elemental analysis. Additionally, it has been shown through X-ray diffraction and DSC that the encapsulated molecules remain in an amorphous state, and the protective function of the loading was demonstrated through thermogravimetry by the decrease in the rate of the thermal decomposition reaction of the drug-loaded material ($\Delta m_{600–850\ °C}$). Finally, the HPLC–MS/MS method developed was proven to be precise and accurate for the determination of prednicarbate in the receiving fluid samples collected during the in vitro release test using Franz diffusion cells.

Keywords SBA-15 · Prednicarbate · Thermal analysis · Nitrogen isotherms · HPLC–MS/MS

✉ Gabriel Lima Barros de Araujo
gabriel.araujo@usp.br

[1] Departamento de Farmácia, Faculdade de Ciências Farmacêuticas, Universidade de São Paulo, São Paulo, SP, Brazil

[2] Center for Skin Biology at Stiefel, a GSK company, Research Triangle Park, NC, USA

[3] Centro de Ciência e Tecnologia de Materiais do Instituto de Pesquisas Energéticas e Nucleares (IPEN), Universidade de São Paulo, São Paulo, SP, Brazil

[4] Departamento de Mineralogia e Geotectônia, Instituto de Geociências, Universidade de São Paulo, São Paulo, SP, Brazil

[5] Departamento de Química Fundamental, Instituto de Química, Universidade de São Paulo, São Paulo, SP, Brazil

Introduction

Different pharmaceutical platforms have been developed to obtain modified drug release systems able to overcome issues related to clinical efficacy, adverse events, and chemical or physical stability. Mesoporous silica matrices have been studied for this purpose due to their specific characteristics: pore size (2–50 nm) and its architecture; extensive surface area (400–1500 $m^2\ g^{-1}$) and pore volume (up to 2.2 $cm^3\ g^{-1}$) [1, 2]; ability to undergo silanol functionalization, yielding to a modified host–guest chemical interaction during adsorption process, as well as the capacity to better control the drug diffusion profile, a highly desirable characteristic for drug delivery systems [1, 3–14]. Previous studies have evaluated the modified release of a large variety of poorly water-soluble substances, demonstrating the successful use of SBA-15 as a carrier material, which is characterized by high surface area, adequate pore volumes, narrow pore size distribution, and non-toxic nature [6, 15–19]. Furthermore, the loading of drugs in mesoporous silica can have a protective effect on the molecule, resulting in the improvement of its chemical stability, as observed by Qu and co-workers using thermogravimetry to evaluate captopril encapsulated in MCM-41 [20]. Prednicarbate is a non-halogenated corticosteroid, double-ester derivative of prednisolone, practically insoluble in water and with high anti-inflammatory activity. It has been widely used for the treatment for atopic

Published online: 08 August 2015

dermatitis in patients whose risk/benefit ratio is high [21], despite its potential to cause severe adverse events, especially during chronic use [22–27]. Thus, the development of a silica-based system for this drug can increase its chemical stability and provide a better release profile and minimize its metabolism by the cutaneous esterases, potentially resulting in a longer therapeutic action and reduction in the daily dose, and consequently decrease frequency of adverse events such as skin thinning [25, 28].

In the present work, a pharmaceutically acceptable procedure to load mesoporous SBA-15 silica with prednicarbate was described and fully characterized to assess its influence on drug stability and its release rate when incorporated in a cream formulation.

Materials and methods

Materials

Prednicarbate (Fig. 1), substance with a molecular mass and formula of 488.58 g mol^{-1} and $C_{27}H_{36}O_8$, respectively, 99.9 % of purity, was obtained from Hawon Biochemical Science Co. Ltd. The silica material (SBA-15) used in the loading process was synthesized according to Matos et al. [29]. For HPLC–MS/MS analysis, HPLC-grade acetonitrile obtained from J.T.Baker and LC–MS-grade formic acid (purity >99 %) obtained from Thermo Scientific were used. Ethanol (purity >99.5 %, J.T.Baker) was used to prepare the receiving fluid in the in vitro release study. Purified water used as component of the receiving fluid and for chromatographic analysis was obtained from a Milli-Q Integral Water Purification system (EMD Millipore). The excipients of the placebo formulation were listed in Neto et al. [21]. The placebo formulation, a cream of low viscosity and white color, was donated by Stiefel Laboratories Ltd., Brazil.

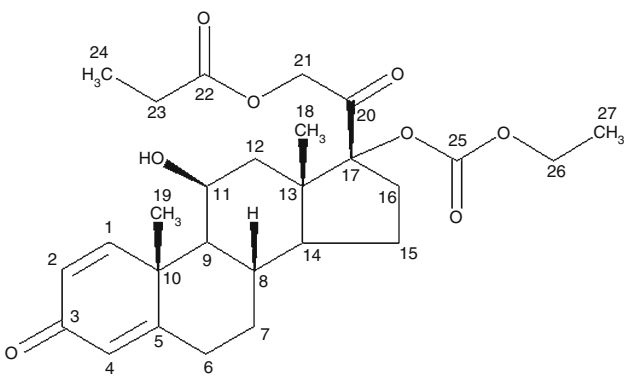

Fig. 1 Chemical structure of prednicarbate

Drug loading and release profile

The loading procedure of SBA-15 with prednicarbate was carried out by adding 500 mg of the drug in a 250-mL volumetric flask and filling the volume with ethanol (99.5 %, J.T.Baker), resulting in a drug concentration of 5 mg mL^{-1}. Ethanol was chosen because it is a safe, non-toxic solvent, in which prednicarbate is readily soluble. An amount of 500 mg of silica was added into the same volumetric flask to obtain a proportion 1:1 drug/SBA-15 (mass/mass). Afterward, the suspension was brought to equilibrium under gentle stirring at 25 °C for 24 h [5]. Subsequently, the suspension was centrifuged for 4 min at 4000 rpm. The remaining drug in the supernatant phase (drug in solution, not incorporated into the SBA-15) was discarded. The powder obtained (pred/SBA-15 sample) was then dried at 80 °C for 2 h, and the amount of drug adsorbed in the SBA-15 was determined by the depletion method.

After the characterization stage of the drug-loaded silica (pred/SBA-15), an appropriate amount of this sample was incorporated into a placebo cream formulation to obtain 0.25 % concentration (mass/mass) of prednicarbate, similarly to the commercial product available [25]. A separate sample of the same placebo formulation was used to prepare a cream with prednicarbate dissolved in ethanol, also resulting in a final drug concentration of 0.25 %. Both semisolid formulations were used in the in vitro release study, which was performed using Franz diffusion cells equipped with an autosampler (Microette® Hanson Research, model 57-6A-S). Recirculating water baths were set at 32 °C, and 12 Franz diffusion cells, each one with a dosing area of 1.77 cm^2 and a volume of 7 mL, were used. The study protocol followed the Guidance for Industry: Nonsterile Semisolid Dosage Forms [30]. The diffusion cells were filled with a receptor medium (continuously stirred at 300 rpm) of ethanol/water (1:1, v/v), which was selected to ensure sink conditions throughout the experiment [31–34]. A synthetic hydrophilic polysulfone membrane (TUFFRYN®; 47 mm of diameter and pore size of 0.45 μm) was placed on top of each diffusion cell. Six diffusion cells were dosed with 260 mg of the cream containing the pred/SBA-15 sample and the other six cells with the cream containing prednicarbate only. At 0.5, 1, 2, 4, 6, 8, 12, 18, and 24 h, an aliquot of 1.0 mL was taken from the receptor compartment and immediately replenished by the same volume of fresh receiving fluid. The concentration of prednicarbate in the aliquots was determined by a validated HPLC–MS/MS method, and the results were plotted against time in order to characterize the prednicarbate release profile in both formulations [35, 36].

Characterization of the materials

Thermogravimetry (TG) and thermogravimetry derivative (DTG) curves were obtained with a thermobalance model TGA-51 (Shimadzu, Japan), using platinum pans with about 25 mg of sample, under air atmosphere (50 mL min^{-1}), at a heating rate (β) of 10 °C min^{-1}, from 25 to 900 °C. Differential scanning calorimetry (DSC) analysis was carried out in a DSC-50 cell (Shimadzu), using aluminum pans with about 2 mg of sample, under dynamic nitrogen (N_2) atmosphere (100 mL min^{-1}), heated (β) at 10 °C min^{-1} from 25 to 600 °C. The DSC cell was calibrated with indium (melting point 156.6 °C and $\Delta H = 28.7$ J g^{-1}) and zinc (melting point 419.6 °C and $\Delta H = 115.8$ J g^{-1}) standards [37].

FTIR spectra of prednicarbate, SBA-15, and sample after the loading process (pred/SBA-15) were recorded at room temperature in the 4000–400 cm^{-1} range. All measured samples were dried, and the powders were mixed with KBr and pressed to a plate for measurement by FTIR spectroscopy. Carbon, hydrogen, and nitrogen contents were determined by elemental analysis using a PerkinElmer analyzer (Model 2400).

The nitrogen adsorption/desorption isotherms were obtained with a Micromeritics equipment model ASAP 2010 pore analyzer set at −196.15 °C under continuous adsorption conditions. The Brunauer–Emmett–Teller (BET) method was used to calculate the surface area (S_{BET}), and the Barrett–Joyner–Halenda (BJH) method was used to calculate pore size diameter and pore volume distribution (V).

The surface morphology of the SBA-15 particles was carried out before and after the loading process by scanning electronic microscopy (SEM) (JEOL equipment, model JSM 7401F).

The X-ray diffraction (XRD) patterns were obtained on a Siemens, model D5000, with tube of Cu Kα, in the range of 3–65° (2θ) and 1 s of pass time, using the powder XRD method.

HPLC–MS/MS conditions

The high-performance liquid chromatography (HPLC) apparatus used was an 1100 series (Agilent Technologies, USA) equipped with a G1311A quaternary pump, a G1315B degasser, a G1313A autosampler, and a G1316A column thermostat. The HPLC was in tandem with a hybrid triple quadruple mass spectrometer model AB SCIEX API 4000 QTRAP (AB SCIEX, USA). The validated HPLC–MS/MS method was adequately sensitive for the analysis of receiving fluid samples and selective toward prednicarbate quantification. Data acquisition and processing were performed using the software Analyst version 1.4.2. The reversed-phase chromatographic analysis was performed at 25 °C on a Pursuit 50 mm × 2.0 mm column packed with 5 μm C_{18} particles (Varian, USA). The mobile phase used was a mixture of water/acetonitrile (2:8, v/v) with 0.1 % of formic acid, with an isocratic elution at a flow rate of 0.3 mL min^{-1} and injection volume of 5.0 μL. Electrospray ionization in positive mode (ESI+) was selected for the analysis of the compound, with a capillary voltage of 5500 V, desolvation temperature set at 600 °C, and curtain gas (air) and desolvation gas (nitrogen) flows set, respectively, at 1.38 and 3.35 bar. The declustering potential (DP) and entrance potential (EP) were, respectively, 51 and 10 V, and the dwell time was 250 ms. Ultrapure nitrogen was used as a collision gas and set at 6 a.u. The collision energy (CE) applied was 13 and 17 eV, respectively, for each multiple reaction monitoring transitions selected (MRM mode, m/z 489.5 > 471.3, and m/z 489.5 > 381.2). Calibration curves for quantitative analysis used the transition m/z 489.5 > 381.2 and were plotted using weighted ($1/x^2$) linear least squares regression [38, 39]. The collision cell exit potential (CXP) was 8 and 16 V for each product ion monitored, respectively, m/z 471.3 and 381.2. The matrix effect (using placebo solution), linearity, precision, accuracy, limit of quantification (LOQ), and limit of detection (LOD) were assessed during the analytical method validation [34, 40–43].

Results and discussion

Characterization of the materials

The results obtained by thermogravimetry (Fig. 2) of the sample after the loading process (pred/SBA-15) showed a mass loss of 5.48 % between 105 and 850 °C, indicating the presence of adsorbed drug on the silica [44–47].

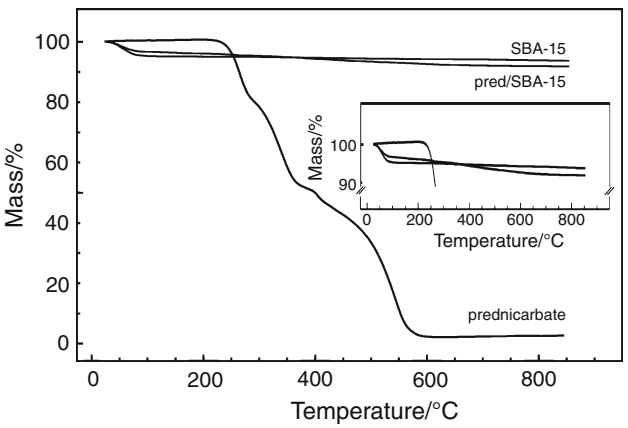

Fig. 2 TG curves of SBA-15, pred/SBA-15, and prednicarbate

The comparative analysis between TG curves (Fig. 2) demonstrated a decrease in the rate of the thermal decomposition reaction of the adsorbed drug. Moreover, the presence of drug in the silica-loaded sample was suggested by an approximated 20 % mass loss observed in the region where the isolated samples (either SBA-15 or drug alone) did not show any thermal event ($\Delta m_{600–850\ °C}$). These results can be attributed to the protective function of the loading in SBA-15 [10, 20].

The comparative assessment of the FTIR spectra (Fig. 3) and the elemental analysis results (Table 1) showed the presence of prednicarbate in the sample generated through the loading process [47]. The 3.1 % of organic material (carbon percentage) detected in the drug-loaded sample (Table 1) corresponded to approximately 4.64 % of prednicarbate (mass/mass).

The SBA-15 and prednicarbate spectra (Fig. 3) showed a stretching band at 3450 cm^{-1}, corresponding to νOH groups. The FTIR spectrum of SBA-15 also showed intense typical bands around 1100 and 1200 cm^{-1}, which are characteristic of silica, as well as other bands relative to the bending modes of hydroxyl groups at 1630 cm^{-1} and at 950 cm^{-1} characteristic of the vibrations of Si–OH of terminal hydroxyl groups (silanols), which have an important role in the stability of the drug in the matrix. It was also observed in the SBA-15 spectrum a band at 800 cm^{-1}, corresponding to the bending vibrations of the Si–O, and another at approximately 470 cm^{-1} related to the bridging bending modes of the O–Si–O [48].

The FTIR spectrum of pred/SBA-15 sample (Fig. 3) showed an absorption band assigned to the C=O group (νC=O) at 1750 cm^{-1}, characteristic of the ester (C_{22}) and carbonate (C_{25}) groups. The intensification of typical silica bands between 1300 and 1100 cm^{-1} region validated the presence of absorption bands at 1280 and 1083 cm^{-1}, assigned to asymmetric stretching of C–O (ν_{as} C–O) in the carbonate group and symmetric stretching of C–O (ν_s C–O) in the ester group, respectively. In the same spectrum at 1650 cm^{-1}, two absorption bands partially overlapping were observed at 1629 cm^{-1}, which is characteristic of silica, and the other at 1652 cm^{-1} assigned to the stretching C=O group (νC=O), characteristic of the semiquinone moiety (C_3) of prednicarbate [37]. These observations combined helped confirming the presence of prednicarbate in the drug-loaded SBA-15 sample [49].

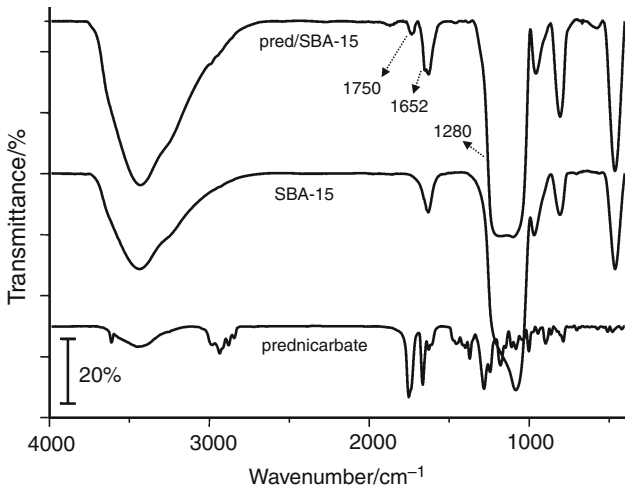

Fig. 3 FTIR spectra of pred/SBA-15, SBA-15, and prednicarbate

Table 1 Elemental analysis results of the SBA-15 silica, prednicarbate, and sample from loading process (pred/SBA-15)

Sample	Carbon/%	Hydrogen/%	Nitrogen/%
SBA-15	0.1	0.4	0.2
Prednicarbate	66.2	7.6	0.1
pred/SBA-15	3.1	1.6	0.1

Figure 4 shows the N_2 adsorption/desorption isotherms and pore size distribution of silica type SBA-15 and the sample obtained through the loading process (pred/SBA-15). These materials exhibit IUPAC type IV isotherm with apparent hysteresis loop between 0.6 and 0.8 of relative pressure (p/p_0), indicative of a narrow distribution of mesoporous in the frameworks and characteristic of a SBA-15 of good quality [6, 29, 50, 51]. The specific surface area was evaluated using BET method (S_{BET}). The pore size (diameter) and pore volume distribution (V) were also measured before and after the loading of prednicarbate using BJH method (Table 2). The S_{BET} and V values decreased, respectively, 24 and 16 % as a result of lining of mesopores by organic drug molecules (Table 2)

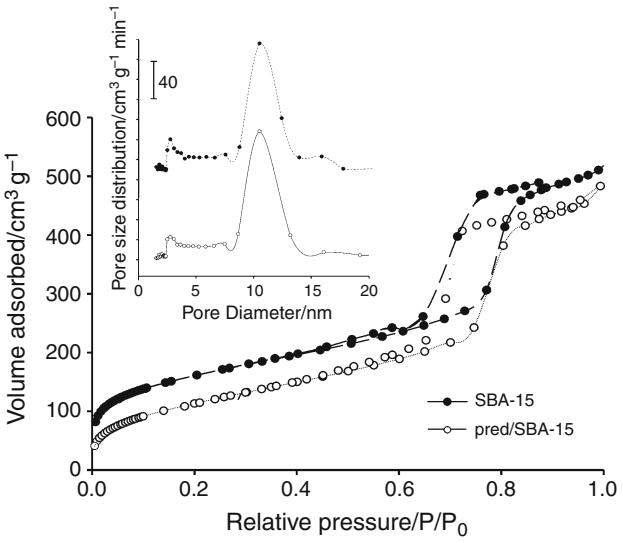

Fig. 4 Nitrogen adsorption/desorption isotherms results of SBA-15 and pred/SBA-15

Table 2 Structural properties of the silica before (SBA-15) and after loading process (pred/SBA-15)

Sample	Particle morphology	Particle size/μm	Pore diameter/nm	S_{BET}/m^2 g^{-1}	V/cm^3 g^{-1}
SBA-15	Rod-like	1.0–2.0	10.08	590	0.91
pred/SBA-15	Rod-like	1.0–2.0	10.08	451	0.76

[12, 47, 49, 52]. However, it was not observed any change in the silica pore size distribution after the loading process, suggesting that the drug molecules are packed inside the pore and not uniformly distributed on the inner surfaces [5]. These results associated with the observed shift of the nitrogen isotherm after loading (Fig. 4), originated by the reduction in total nitrogen amount adsorbed under different relative pressure values [6], confirm that the drug was introduced inside the channels of the SBA-15, validating the prednicarbate encapsulation [8, 20].

The SEM images obtained for SBA-15 before and after the loading process (Fig. 5) showed similar macrostructure, with a rod-like morphology and the majority of the particle sizes ranging from 1.0 to 2.0 μm [42, 43]. The XRD patterns of prednicarbate crystals, SBA-15, and pred/SBA-15 samples are displayed in Fig. 6. Diffraction peak characteristics of prednicarbate crystals or other crystalline phase were not observed for the drug-loaded material, indicating that no crystallization process occurred to the molecules adsorbed inside the pores [5, 8, 10, 53]. The DSC curve of the drug-loaded sample did not display an endothermic event between 175 and 200 °C, which is the characteristic of the melting of the drug crystal [21] (Fig. 7); this also indicated the inexistence of any crystalline drug phase after the loading process [53].

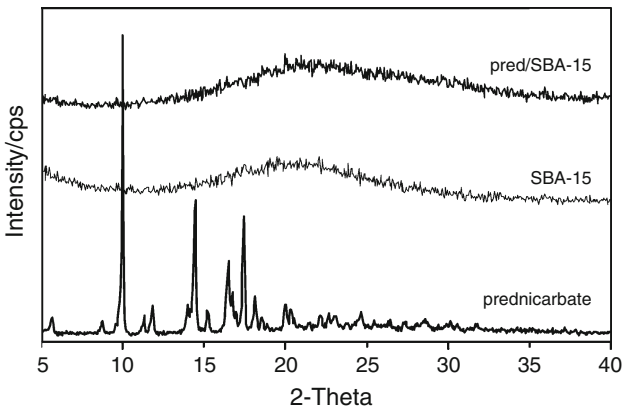

Fig. 6 XRD diffraction patterns (wide angle) obtained from pred/SBA-15, SBA-15, and prednicarbate

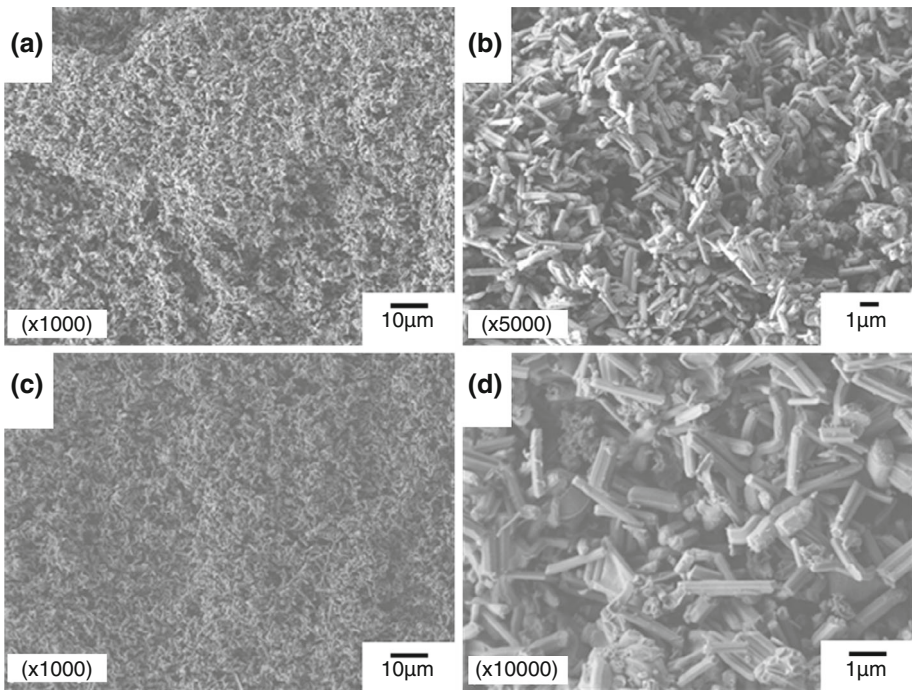

Fig. 5 SEM images of SBA-15 (**a**, **b**) and pred/SBA-15 (**c**, **d**) microparticles

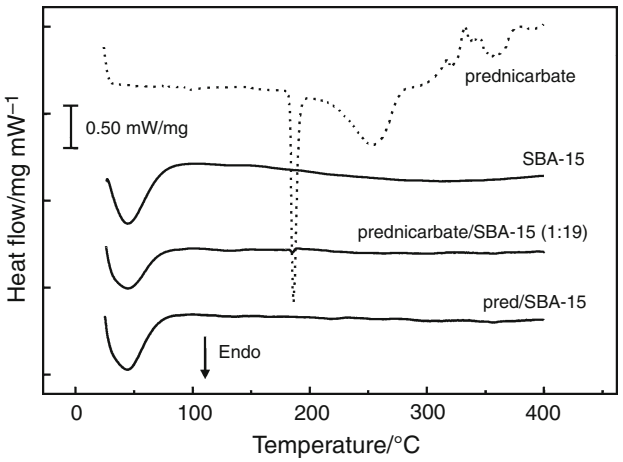

Fig. 7 DSC curves of prednicarbate, SBA-15, physical mixture between prednicarbate and SBA-15 (1:19), and pred/SBA-15

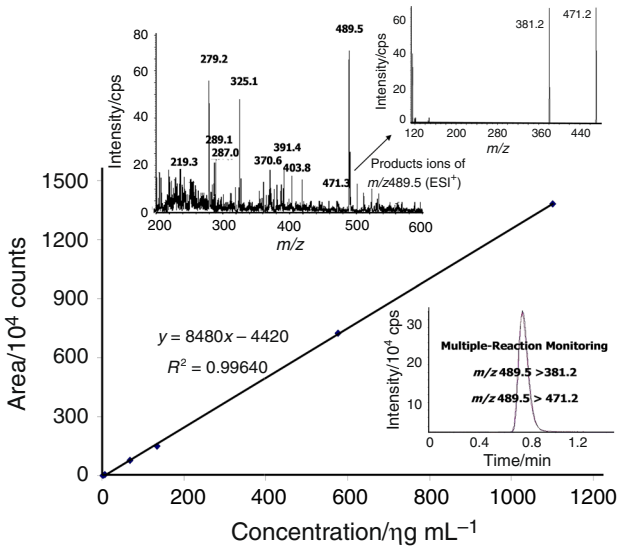

Fig. 8 Scan mode mass spectrum and product ion mass spectrum of prednicarbate molecular ion (*m/z* 489.5), and calibration curve by MRM mode (transition 489.5 > 381.2) using HPLC–MS/MS

Analytical development and validation of the HPLC–MS/MS method

The HPLC–MS/MS method was developed and validated for the quantification of prednicarbate in the receiving fluid samples collected during the in vitro release test. Mass spectrum of the prednicarbate solution (50 ng mL^{-1} dissolved in receptor medium) was obtained in full scan positive mode using electrospray ionization (ESI+). A high abundance positive molecular ion with *m/z* 489.5 was observed, indicating the presence of the compound of interest. The product ion mass spectrum of *m/z* 489.5 obtained using collision energy (CE) set at 13 and 17 eV resulted, respectively, in *m/z* 471.2 and 381.2 as major fragments, which are consistent with the structure of the compound. The determination of both transitions by MRM mode (*m/z* 489.5 > 471.3 and 489.5 > 381.2) for the receiving fluid samples confirmed the presence of the prednicarbate [38, 39]. The calibration curve for HPLC–MS/MS analysis was plotted for concentrations ranging from 1.5 to 1380 ng mL^{-1} (standards dissolved in the receptor medium), using weighted ($1/x^2$) linear least squares regression, smooth factor of 1.0, and the transition 489.5 > 381.2. The coefficient of determination (R^2) ≥0.99 indicated a linear correlation between the drug concentrations and their peak areas over a three-log concentration range, with recovery values (triplicate measurements) for each concentration between 90 and 110 %. The regression equation, R^2 value, and mass spectra are displayed in Fig. 8.

The matrix effect was evaluated using a solution of placebo formulation dissolved in the receiving fluid. It was not observed any ion suppression or enhancement of the protonated drug (*m/z* 489.5) when placebo solution was injected directly in the ion source in combination with chromatographic analysis of the prednicarbate solution [39–41, 43]. The precision and accuracy of the method were determined by the analysis of three nominal concentrations (six replicates per concentration): 10.9, 223, and 632 ng mL^{-1}. The accuracy was determined comparing the mean measured concentration with the nominal values and the precision by relative standard deviation of the replicates (RSD). The results (Table 3) indicated that the HPLC–MS/MS method is precise (RSD ≤ 5 %) and accurate (recovery between 90 and 110 %) for quantitative determination of prednicarbate in receiving fluid samples.

The LOD value, defined as the sample concentration resulting in a peak area of three times the noise level, and the LOQ value, defined as the lowest drug concentration which can be determined with accuracy and precision, were, respectively, 0.87 and 1.50 ng mL^{-1} [34, 42].

Release profile

The in vitro release of prednicarbate, either incorporated freely in the placebo cream formulation or loaded into SBA-15, was performed with six replicates of each test article, using Franz diffusion cells and synthetic polysulfone membranes. The drug-loaded silica had approximately 5 % of adsorbed prednicarbate into the SBA-15, meaning that each diffusion cell was dosed with 648.7 μg of drug (260 mg of formulation applied), which is equivalent to a 0.25 % concentration [25]. The release profiles of both semisolid formulations are displayed in Fig. 9, which shows the cumulative amount of prednicarbate (μg) over time (h) (Table 4).

Table 3 Precision and accuracy of the HPLC–MS/MS method for the determination of prednicarbate in the receptor medium ($n = 6$)

Theoretical concentration/ηg mL^{-1}	Concentration found (mean ± SD)/ηg mL^{-1}	Precision (RSD)/%	Accuracy (mean ± SD)/%
10.9	11.3 ± 0.22	1.9	103.0 ± 1.97
223	232 ± 2.45	1.1	104.1 ± 1.10
632	623 ± 4.67	0.8	98.6 ± 0.74

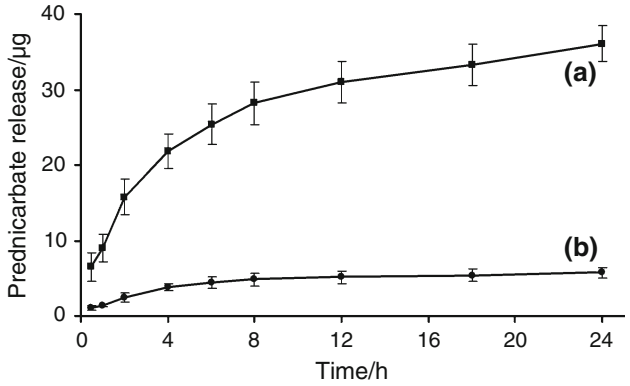

Fig. 9 Cumulative release rates of prednicarbate incorporated freely in the cream formulation (**a**) and after being loaded into SBA-15 (**b**)

Table 4 Cumulative amount (µg) of prednicarbate released during in vitro test (six replicates per time point)

Time/ hours	Prednicarbate incorporated freely (mean ± SD)/µg	Prednicarbate loaded into SBA-15 (mean ± SD)/µg
0.5	6.49 ± 1.911	1.10 ± 0.263
1.0	9.02 ± 1.803	1.38 ± 0.215
2.0	15.80 ± 2.362	2.45 ± 0.587
4.0	21.86 ± 2.299	3.86 ± 0.455
6.0	25.36 ± 2.678	4.38 ± 0.776
8.0	28.17 ± 2.830	4.84 ± 0.818
12.0	31.01 ± 2.779	5.16 ± 0.869
18.0	33.29 ± 2.728	5.41 ± 0.815
24.0	36.09 ± 2.354	5.75 ± 0.731

The lower reproducibility of the results observed in the first 2 h of the release profile was likely due to the system reaching its steady state. The comparison of the release profile of both formulations showed significant difference (Fig. 9). The cream containing drug loaded in the SBA-15 showed a cumulative amount sixfold lower than the formulation with free drug. The release rate was also lower during the course of the experiment, demonstrating a modified release of prednicarbate when loaded in the SBA-15 [6, 19, 20]. The release rate of drug-loaded in the first 6 h was approximately fourfold higher than the rate from 6 to 24 h. This pronounced difference in the rates, representing around 78 % of the total drug released in the first 6 h, is attributed to easy dissolution and diffusion of the drug packed inside the pores and not adsorbed on the inner surface of them [5, 6]. The large pore sizes of the SBA-15 (10 nm) might reduce steric diffusion resistance, contributing also to this faster release rate at the beginning of the experiment [20]. The presence of a small amount of prednicarbate adsorbed on the external surfaces of silica particles may have also contributed to this higher initial rate of drug release [7]. The very slow release pattern of the sample containing drug-loaded SBA-15 was observed after 6 h of testing (Fig. 9). This lower release rate can be attributed to the presence of micropores in the SBA-15 [6, 51], displayed in Fig. 4. A fraction of the micropores presented in the SBA-15 is associated with the walls of primary mesopores, resulting in longer diffusion paths for the drug due to interconnecting channels [29].

According to the results obtained, the loading of the prednicarbate in SBA-15 provides a better chemical protection of the substance as well as a controlled release of the drug [26, 27]. These two characteristics combined have the potential to increase the clinical efficacy of prednicarbate and improve the safety profile of this corticosteroid.

Conclusions

The results demonstrated that prednicarbate can be loaded into SBA-15 mesoporous silica using ethanol, a safe and non-toxic solvent, through the process described herein. The FTIR spectrum of the drug-loaded sample displayed characteristic absorption bands of prednicarbate, confirming the presence of this molecule after the loading. The decrease in the surface area and mesoporous volume observed in the nitrogen adsorption/desorption isotherms of the drug-loaded material, associated with the shift observed in these isotherms and maintenance of the pore size, indicated an efficacious drug encapsulation process into the SBA-15. These results also suggested a preferred packing of the molecules inside the pores, instead of uniform adsorption on the inner surfaces, as described previously. Thermogravimetric and elemental analysis results confirmed each other, suggesting around 5 % of drug content

in the loaded material. The reduction observed by thermogravimetry in the rate of thermal decomposition reaction of the drug in this material confirmed the protective function to the loading. Moreover, it has been shown through X-ray diffraction and DSC that the encapsulated molecules remain in an amorphous state. The release profile obtained for the drug-loaded SBA-15 has the potential to reduce the frequency of typical adverse events associated with this corticosteroid, mainly due to a modified release rate, as well as an improved chemical protection of this molecule, with the potential to decrease drug metabolism by cutaneous esterases. In conclusion, the SBA-15 silica proved to be a material with a high potential for the use in topical formulations as a carrier of poorly water-soluble drugs of dermatological interest.

Acknowledgements The authors acknowledge the Conselho Nacional de Desenvolvimento Científico e Tecnológico (CNPq), Coordenação de Aperfeiçoamento de Pessoal de Nível Superior (CAPES), Fundação de Amparo à Pesquisa do Estado de São Paulo (FAPESP), and Stiefel Laboratories for the financial support.

References

1. Wang Y, Zhao Q, Han N, Bai L, Li J, Liu J, et al. Mesoporous silica nanoparticles in drug delivery and biomedical applications. Nanomed Nanotechnol Biol Med. 2015;11(2):313–27.
2. Cides da Silva LC, Araujo GLB, Segismundo NR, Moscardini EF, Mercuri LP, Cosentino IC, et al. DSC estimation of structural and textural parameters of SBA-15 silica using water probe. J Therm Anal Calorim. 2009;97(2):701–4. doi:10.1007/s10973-009-0334-7.
3. Kresge C, Leonowicz M, Roth W, Vartuli J, Beck J. Ordered mesoporous molecular sieves synthesized by a liquid-crystal template mechanism. Nature. 1992;359(6397):710–2.
4. Vartuli J, Roth W, Beck J, McCullen S, Kresge C. The synthesis and properties of M41S and related mesoporous materials. Berlin: Synthesis. Springer; 1998. p. 97–119.
5. Charnay C, Bégu S, Tourné-Péteilh C, Nicole L, Lerner D, Devoisselle J-M. Inclusion of ibuprofen in mesoporous templated silica: drug loading and release property. Eur J Pharm Biopharm. 2004;57(3):533–40.
6. Doadrio A, Sousa E, Doadrio J, Pariente JP, Izquierdo-Barba I, Vallet-Regı M. Mesoporous SBA-15 HPLC evaluation for controlled gentamicin drug delivery. J Control Release. 2004;97(1):125–32.
7. Salonen J, Laitinen L, Kaukonen A, Tuura J, Björkqvist M, Heikkilä T, et al. Mesoporous silicon microparticles for oral drug delivery: loading and release of five model drugs. J Control Release. 2005;108(2):362–74.
8. Heikkilä T, Salonen J, Tuura J, Hamdy M, Mul G, Kumar N, et al. Mesoporous silica material TUD-1 as a drug delivery system. Int J Pharm. 2007;331(1):133–8.
9. Wang F, Hui H, Barnes TJ, Barnett C, Prestidge CA. Oxidized mesoporous silicon microparticles for improved oral delivery of poorly soluble drugs. Mol Pharm. 2009;7(1):227–36.
10. Moritz M. Modified SBA-15 as the carrier for metoprolol and papaverine: adsorption and release study. J Solid State Chem. 2011;184(7):1761–7.
11. Santos H, Salonen J, Bimbo L, Lehto V-P, Peltonen L, Hirvonen J. Mesoporous materials as controlled drug delivery formulations. J Drug Deliv Sci Technol. 2011;21(2):139–55.
12. Pang J, Zhao L, Zhang L, Li Z, Luan Y. Folate-conjugated hybrid SBA-15 particles for targeted anticancer drug delivery. J Colloid Interface Sci. 2013;395:31–9.
13. Chen L, Zheng Z, Wang J, Wang X. Mesoporous SBA-15 end-capped by PEG via L-cystine based linker for redox responsive controlled release. Microporous Mesoporous Mater. 2014;185:7–15.
14. Rodríguez-Estupiñán P, Giraldo L, Moreno-Piraján JC. Calorimetric study of amino-functionalised SBA-15. J Therm Anal Calorim. 2015;121(1):1–8.
15. Vallet-Regi M, Ramila A, Del Real R, Pérez-Pariente J. A new property of MCM-41: drug delivery system. Chem Mater. 2001;13(2):308–11.
16. Lai C-Y, Trewyn BG, Jeftinija DM, Jeftinija K, Xu S, Jeftinija S, et al. A mesoporous silica nanosphere-based carrier system with chemically removable CdS nanoparticle caps for stimuli-responsive controlled release of neurotransmitters and drug molecules. J Am Chem Soc. 2003;125(15):4451–9.
17. Rámila A, Munoz B, Pérez-Pariente J, Vallet-Regí M. Mesoporous MCM-41 as drug host system. J Sol–Gel Sci Technol. 2003;26(1–3):1199–202.
18. Song S-W, Hidajat K, Kawi S. Functionalized SBA-15 materials as carriers for controlled drug delivery: influence of surface properties on matrix-drug interactions. Langmuir. 2005;21(21):9568–75.
19. Y-f Zhu, J-l Shi, Y-s Li, H-r Chen, W-h Shen, X-p Dong. Storage and release of ibuprofen drug molecules in hollow mesoporous silica spheres with modified pore surface. Microporous Mesoporous Mater. 2005;85(1):75–81.
20. Qu F, Zhu G, Huang S, Li S, Sun J, Zhang D, et al. Controlled release of Captopril by regulating the pore size and morphology of ordered mesoporous silica. Microporous Mesoporous Mater. 2006;92(1):1–9.
21. Neto H, Novák C, Matos J. Thermal analysis and compatibility studies of prednicarbate with excipients used in semi solid pharmaceutical form. J Therm Anal Calorim. 2009;97(1):367–74.
22. Cornell R, Cherill R, Abrams B. Safety of prednicarbate emollient cream 0.1 % and ointment 0.1 %, nonhalogenated, midpotency topical steroid formulations. J Geriatr Dermatol. 1994;2:57–65.
23. Fleischer Jr AB. Atopic dermatitis. Perspectives on a manageable disease. Postgrad Med. 1999;106:49–55.
24. Fennessy M, Coupland S, Popay J, Naysmith K. The epidemiology and experience of atopic eczema during childhood: a discussion paper on the implications of current knowledge for health care, public health policy and research. J Epidemiol Community Health. 2000;54(8):581–9.
25. Gupta A, Chow M. Prednicarbate (dermatop): a review. J drugs dermatol JDD. 2003;3(5):553–6.
26. Lange K, Gysler A, Bader M, Kleuser B, Korting HC, Schäfer-Korting M. Prednicarbate versus conventional topical glucocorticoids: pharmacodynamic characterization in vitro. Pharm Res. 1997;14(12):1744–9.
27. Lange K, Kleuser B, Gysler A, Bader M, Maia C, Scheidereit C, et al. Cutaneous inflammation and proliferation in vitro: differential effects and mode of action of topical glucocorticoids. Skin Pharmacol Physiol. 2000;13(2):93–103.
28. Korting HC, Unholzer A, Schäfer-Korting M, Tausch I, Gassmueller J, Nietsch K-H. Different skin thinning potential of equipotent medium-strength glucocorticoids. Skin Pharmacol Physiol. 2002;15(2):85–91.

29. Matos JR, Mercuri LP, Kruk M, Jaroniec M. Toward the synthesis of extra-large-pore MCM-41 analogues. Chem Mater. 2001;13(5):1726–31.
30. FDA. Nonsterile semisolid dosage forms. Scale-up and post-approval changes: chemistry, manufacturing and controls; In Vitro release testing and In Vivo Bioequivalence documentation. 1997.
31. Choi HK, Flynn GL, Amidon GL. Percutaneous absorption and dermal delivery of cyclosporin A. J Pharm Sci Us. 1995;84(5):581–3.
32. Guo J, Ping Q, Sun G, Jiao C. Lecithin vesicular carriers for transdermal delivery of cyclosporin A. Int J Pharm. 2000;194(2):201–7.
33. Boinpally RR, Zhou S-L, Devraj G, Anne PK, Poondru S, Jasti BR. Iontophoresis of lecithin vesicles of cyclosporin A. Int J Pharm. 2004;274(1):185–90.
34. Chang X-L, Chen H-B, Zhao X-Z, Gao Z-H, Xu H-B, Yang X-L. High-performance liquid chromatography determination of triptolide in vitro permeation studies. Anal Chim Acta. 2005;534(2):215–21.
35. Lopes LB, Collett JH, Bentley MVL. Topical delivery of cyclosporin A: an in vitro study using monoolein as a penetration enhancer. Eur J Pharm Biopharm. 2005;60(1):25–30.
36. Winkler A, Müller-Goymann CC. The influence of topical formulations on the permeation of 5-aminolevulinic acid and its n-butyl ester through excised human stratum corneum. Eur J Pharm Biopharm. 2005;60(3):427–37.
37. Neto HS, Barros FAP, de Sousa Carvalho FM, Matos JR. Thermal analysis of prednicarbate and characterization of thermal decomposition product. J Therm Anal Calorim. 2010;102(1):277–83.
38. Lagerwerf FM, van Dongen WD, Steenvoorden RJ, Honing M, Jonkman JH. Exploring the boundaries of bioanalytical quantitative LC–MS–MS. TrAC Trends Anal Chem. 2000;19(7):418–27.
39. Niessen W. Progress in liquid chromatography–mass spectrometry instrumentation and its impact on high-throughput screening. J Chromatogr A. 2003;1000(1):413–36.
40. Matuszewski B, Constanzer M, Chavez-Eng C. Strategies for the assessment of matrix effect in quantitative bioanalytical methods based on HPLC-MS/MS. Anal Chem. 2003;75(13):3019–30.
41. Taylor PJ. Matrix effects: the Achilles heel of quantitative high-performance liquid chromatography–electrospray–tandem mass spectrometry. Clin Biochem. 2005;38(4):328–34.
42. Kolodsick KJ, Phillips H, Feng J, Molski M, Kingsmill CA. Enhancing drug development by applying LC–MS–MS for cleaning validation in manufacturing equipment. Pharm Technol. 2006;30(2):56.
43. Xu RN, Fan L, Rieser MJ, El-Shourbagy TA. Recent advances in high-throughput quantitative bioanalysis by LC–MS/MS. J Pharm Biomed Anal. 2007;44(2):342–55.
44. Chen J-F, Ding H-M, Wang J-X, Shao L. Preparation and characterization of porous hollow silica nanoparticles for drug delivery application. Biomaterials. 2004;25(4):723–7.
45. Lehto V-P, Vähä-Heikkilä K, Paski J, Salonen J. Use of thermoanalytical methods in quantification of drug load in mesoporous silicon microparticles. J Therm Anal Calorim. 2005;80(2):393–7.
46. Tang Q, Xu Y, Wu D, Sun Y, Wang J, Xu J, et al. Studies on a new carrier of trimethylsilyl-modified mesoporous material for controlled drug delivery. J Controlled Release. 2006;114(1):41–6.
47. Moritz M, Łaniecki M. Application of SBA-15 mesoporous material as the carrier for drug formulation systems. Papaverine hydrochloride adsorption and release study. Powder Technol. 2012;230:106–11.
48. López T, Basaldella E, Ojeda M, Manjarrez J, Alexander-Katz R. Encapsulation of valproic acid and sodic phenytoin in ordered mesoporous SiO 2 solids for the treatment of temporal lobe epilepsy. Opt Mater. 2006;29(1):75–81.
49. Szegedi A, Popova M, Goshev I, Mihály J. Effect of amine functionalization of spherical MCM-41 and SBA-15 on controlled drug release. J Solid State Chem. 2011;184(5):1201–7.
50. Zhao D, Feng J, Huo Q, Melosh N, Fredrickson GH, Chmelka BF, et al. Triblock copolymer syntheses of mesoporous silica with periodic 50–300 angstrom pores. Science. 1998;279(5350):548–52.
51. Kruk M, Jaroniec M, Ko CH, Ryoo R. Characterization of the porous structure of SBA-15. Chem Mater. 2000;12(7):1961–8.
52. Sevimli F, Yılmaz A. Surface functionalization of SBA-15 particles for amoxicillin delivery. Microporous Mesoporous Mater. 2012;158:281–91.
53. Ahern RJ, Hanrahan JP, Tobin JM, Ryan KB, Crean AM. Comparison of fenofibrate–mesoporous silica drug-loading processes for enhanced drug delivery. Eur J Pharm Sci. 2013;50(3):400–9.